

# Effective potential and mass behavior of a self-interacting scalar field theory due to thermal and external electric and magnetic fields effects

M. Loewe<sup>1,2,3</sup>, D. Valenzuela<sup>1</sup> and R. Zamora<sup>4,5</sup>

<sup>1</sup>*Instituto de Física, Pontificia Universidad Católica de Chile, Casilla 306, Santiago 22, Chile.*

<sup>2</sup>*Centre for Theoretical and Mathematical Physics, and Department of Physics, University of Cape Town, Rondebosch 7700, South Africa.*

<sup>3</sup>*Centro Científico-Tecnológico de Valparaíso CCTVAL, Universidad Técnica Federico Santa María, Casilla 110-V, Valparaíso, Chile.*

<sup>4</sup>*Instituto de Ciencias Básicas, Universidad Diego Portales, Casilla 298-V, Santiago, Chile.*

<sup>5</sup>*Centro de Investigación y Desarrollo en Ciencias Aeroespaciales (CIDCA), Fuerza Aérea de Chile, Casilla 8020744, Santiago, Chile.*

In this article we address the subject of finding the behavior of a charged scalar field  $\phi$  under the influence of external constant magnetic and electric fields, perpendicular to each other, including also thermal effects. For this purpose we derive an expression for the corresponding bosonic propagator. As an application, we explore, in the weak field sector, the mass correction for the self-interacting  $\lambda\phi^4$  theory. It turns out that the electric and magnetic fields induce a decreasing of the mass, playing the electric field a more dominant role in comparison with the magnetic field contribution. On the other side, the mass grows with temperature. We also analyzed the phase diagram associated to spontaneous symmetry breaking of the theory, finding inverse magnetic catalysis (IMC) or inverse electric catalysis (IEC) for the cases where only a magnetic field or only an electric field were present, respectively. In both cases we have a scenario where the critical temperature associated to symmetry restoration diminishes as function of the corresponding field strengths. A similar situation happens when both type of fields are simultaneously present. We have dubbed this case as inverse magnetic-electric catalysis (IMEC). Here, both fields cooperate for the occurrence of IMEC, being the role of the electric field, however, more dominant than the influence of the magnetic field for the decreasing of the critical temperature.

Keywords: Bosonic propagator, Effective Models, Electric Fields, Magnetic Fields.

## I. INTRODUCTION

In this article we derive a propagator for a charged scalar field in the presence of constant external magnetic and electric fields. This propagator is used then to explore the mass behavior of the  $\phi$  field, in the frame of a self-interacting  $\lambda\phi^4$  theory, as function of temperature and the external magnetic and electric field strengths, taking both fields simultaneously. As a second application, we analyze the phase diagram of this theory starting from the broken phase. For this purpose we find the effective potential, including the resummation of ring diagrams, finding the dependence of the critical temperature on the external electromagnetic field strengths.

In the existing literature, different aspects concerning the behavior of hadronic parameters and the properties of the QCD phase diagram in the presence of thermal and external magnetic effects have been considered during the last years [1–28]. In [29] we might find general review articles concerning the role of magnetic effects in strongly interacting matter. In particular, it is interesting to mention that it is possible to find inverse magnetic catalysis in the frame of effective models, in agreement with the well known results from the lattice community [30], i.e. the fact that the critical temperature diminishes with the magnetic field strength. We have analyzed this point by a careful discussion of symmetry restoration both in a self-interacting scalar field model as well as in the linear sigma field coupled to quarks, dealing in the last case with chi-

ral symmetry restoration. It turns out that this can only be achieved by going beyond the mean field approximation, through a ring diagram resummation. [31, 32]. A recent review about these facts, including a discussion of thermo-magnetic effects in the Nambu-Jona-Lasinio model, is presented in [33]. A discussion of the effective potential, in the case of a pure external electric field, shows the occurrence of electric anticatalysis for small values of the electric field, whereas catalysis appears for high values of the electric field strength [34, 35]. We also want to mention, in the context of the influence of external fields, a complete different aspect, namely the evolution of the residues of renormalons in this theory under the influence of an electric field which has also recently been addressed by some of us. [36].

In this article we would like to consider the situation or scenario where the effects of both kind of external fields, electric and magnetic, are taken into account. The physical scenario where such a case appears corresponds to peripheral collisions of asymmetric heavy ions. For example, in Au-Cu collisions an electric dipole field is generated due to the imbalance of the number of charged particles (protons) in both nuclei. This field will basically be perpendicular to the magnetic field generated also under such conditions. In [37] we might find an analysis when both types of fields are present, but in a parallel configuration, which corresponds actually to the chiral magnetic effect. For the purpose of analyzing collisions between asymmetric nuclei, however, the configuration

where both fields are perpendicular to each other is the relevant one.

This article is organized as follows. In section II we derive the bosonic propagator in the presence of external constant magnetic and electric fields in a perpendicular configuration relative to each other. We also present the propagator's expansion for the case of weak fields. In section III we make use of the propagator to find the electromagnetic mass correction of the charged scalar field. In section IV we proceed with the discussion of the effective potential at the one loop level, including also ring corrections, finding the behavior of the critical temperature where the symmetry is restored as function of the magnetic and electric field strengths. Finally, in section V we present our conclusions.

## II. THE BOSON PROPAGATOR IN THE PRESENCE OF AN ELECTRIC AND MAGNETIC FIELD

We begin with the proper time representation for a charged boson propagator in the presence of an external electromagnetic field encoded in the  $F^{\mu\nu}$  tensor [38, 39] which is given by

$$D(p) = \int_0^\infty dt e^{-m^2 t} \frac{e^{t p_\mu \left(\frac{\tan(Z)}{Z}\right)^{\mu\nu} p_\nu}}{\sqrt{\det(Z)}}, \quad (1)$$

where  $Z^{\mu\nu} \equiv q F^{\mu\nu} t$ , with  $q$  the electric charge and  $p$  the euclidean four-momentum defined as  $p = (p_4, p_1, p_2, p_3)$ . Our analysis is presented in the Euclidean formulation. As we said in the introduction, we are interested in a configuration where  $\vec{B} \perp \vec{E}$ . Without loss of generality, We assume that  $\vec{B} = B_0 \hat{z}$  and  $\vec{E} = E_0 \hat{x}$  that is

$$F^{\mu\nu} = \begin{bmatrix} 0 & -E_0 & 0 & 0 \\ E_0 & 0 & -B_0 & 0 \\ 0 & B_0 & 0 & 0 \\ 0 & 0 & 0 & 0 \end{bmatrix}. \quad (2)$$

Thus, we can decompose  $F^{\mu\nu}$  as

$$F^{\mu\nu} \equiv E_0 E^{\mu\nu} + B_0 B^{\mu\nu}, \quad (3)$$

where

$$E^{\mu\nu} = \begin{bmatrix} 0 & -1 & 0 & 0 \\ 1 & 0 & 0 & 0 \\ 0 & 0 & 0 & 0 \\ 0 & 0 & 0 & 0 \end{bmatrix} \text{ and } \quad (4)$$

$$B^{\mu\nu} = \begin{bmatrix} 0 & 0 & 0 & 0 \\ 0 & 0 & -1 & 0 \\ 0 & 1 & 0 & 0 \\ 0 & 0 & 0 & 0 \end{bmatrix}. \quad (5)$$

Let us compute the square of  $F^{\mu\nu}$

$$(F^2)^{\mu\nu} = E_0^2 (E^2)^{\mu\nu} + B_0^2 (B^2)^{\mu\nu} + E_0 B_0 S^{\mu\nu}, \quad (6)$$

with

$$(E^2)^{\mu\nu} = \begin{bmatrix} -1 & 0 & 0 & 0 \\ 0 & -1 & 0 & 0 \\ 0 & 0 & 0 & 0 \\ 0 & 0 & 0 & 0 \end{bmatrix}, \quad (7)$$

$$(B^2)^{\mu\nu} = \begin{bmatrix} 0 & 0 & 0 & 0 \\ 0 & -1 & 0 & 0 \\ 0 & 0 & -1 & 0 \\ 0 & 0 & 0 & 0 \end{bmatrix} \text{ and } \quad (8)$$

$$S^{\mu\nu} = \begin{bmatrix} 0 & 0 & 1 & 0 \\ 0 & 0 & 0 & 0 \\ 1 & 0 & 0 & 0 \\ 0 & 0 & 0 & 0 \end{bmatrix}, \quad (9)$$

We find the following relations for the powers of  $F^{\mu\nu}$

$$(F^{2n})^{\mu\nu} = [- (E_0^2 + B_0^2)]^n (F^2)^{\mu\nu} \quad (10)$$

$$(F^{2n+1})^{\mu\nu} = [- (E_0^2 + B_0^2)]^n F^{\mu\nu} \quad \forall n \in \mathbb{N}^0. \quad (11)$$

summarizing, we have

$$(F^0)^{\mu\nu} \equiv \delta^{\mu\nu}, \quad (12)$$

$$(F^{2n})^{\mu\nu} = (-\lambda^2)^n (F^2)^{\mu\nu}, \quad (13)$$

$$(F^{2n+1})^{\mu\nu} = (-\lambda^2)^n F^{\mu\nu} \quad \forall n \in \mathbb{N}^0, \quad (14)$$

where we have defined

$$\lambda^2 \equiv E_0^2 + B_0^2. \quad (15)$$

With these relations, we obtain

$$\begin{aligned} [\cos(Z)]^{\mu\nu} &= \delta^{\mu\nu} + 2 \frac{\sin^2(\frac{1}{2} q \lambda i t)}{\lambda^2} (F^2)^{\mu\nu} \\ &\Rightarrow \det[\cos(Z)] = \cos(q \lambda i t), \end{aligned} \quad (16)$$

and

$$\left[ \frac{\tan(Z)}{Z} \right]^{\mu\nu} = \delta^{\mu\nu} - \left[ \frac{\tan(q \lambda i t)}{q \lambda i t} - 1 \right] \frac{(F^2)^{\mu\nu}}{\lambda^2}. \quad (17)$$

Finally, inserting Eq. (16) and Eq. (17) in Eq. (1), we get

$$\begin{aligned} D(p) &= \int_0^\infty d\tau e^{-\tau(p_3^2 + (\cos(\chi)p_4 + \sin(\chi)p_2)^2 + m^2)} \\ &\quad \times \frac{e^{\frac{\tan(q \lambda i t)}{q \lambda i t} (p_1^2 + (\sin(\chi)p_4 + \cos(\chi)p_2)^2)}}{\cos(q \lambda i t)} \\ &= \int_0^\infty d\tau e^{-\tau(p_3^2 + (\cos(\chi)p_4 + \sin(\chi)p_2)^2 + m^2)} \\ &\quad \times \frac{e^{\frac{\tanh(q \lambda t)}{q \lambda t} (p_1^2 + (\sin(\chi)p_4 + \cos(\chi)p_2)^2)}}{\cosh(q \lambda t)}, \end{aligned} \quad (18)$$

where  $\cos(\chi) \equiv \frac{B_0}{\lambda}$  and  $\sin(\chi) \equiv \frac{E_0}{\lambda}$ .

### A. Weak field expansion of the propagator

In order to find a weak field expansion for the propagator, we follow the ideas presented in [40], and proceed with an expansion for small  $\lambda$  values in Eq. (18) using the expressions

$$\frac{\tanh(x)}{x} \approx 1 - \frac{1}{3}x^2 + \frac{2}{15}x^4 \quad (19)$$

$$\text{sech}(x) \approx 1 - \frac{1}{2}x^2 \quad (20)$$

$$e^x \approx 1 + x. \quad (21)$$

After integrating the above expression in the proper time  $\tau$ , we obtain the expansion of the propagator given in Eq. (18) up to order  $\mathcal{O}(\lambda^4)$

$$D(p) \approx \frac{1}{p^2 + m^2} \quad (22)$$

$$- \frac{(q\lambda)^2}{(p^2 + m^2)^3} \left[ 1 - 2 \frac{p_1^2 + (\sin(\chi)p_4 - \cos(\chi)p_2)^2}{p^2 + m^2} \right] \quad (23)$$

$$- (2q\lambda)^4 \frac{(\sin(\chi)p_4 - \cos(\chi)p_2)^2}{(p^2 + m^2)^6} + \dots \quad (24)$$

Since we want to find an expansion up to the order  $\mathcal{O}(E^2)$  and  $\mathcal{O}(B^2)$ , we will reorganize the previous expression up to this order. Returning to the original variables we obtain

$$\begin{aligned} D(p) &\approx \frac{1}{p^2 + m^2} - \frac{4p_4p_2(qB)(qE)}{(p^2 + m^2)^4} \\ &- \frac{(qE)^2(m^2 + p^2 - 2(p_4^2 + p_1^2))}{(p^2 + m^2)^4} \\ &- \frac{(qB)^2(m^2 + p^2 - 2p_\perp^2)}{(p^2 + m^2)^4}, \end{aligned} \quad (25)$$

where  $p_\perp = (0, p_1, p_2, 0)$ . It is important to avoid  $p_4^2$  terms in the numerator of the above expression. When going into a finite temperature scenario, those terms are cumbersome to be handled. In this way we get

$$\begin{aligned} D(p) &\approx \frac{1}{p^2 + m^2} - \frac{4p_2p_4(qB)(qE)}{(p^2 + m^2)^4} \\ &- \frac{3(qE)^2 + (qB)^2}{(p^2 + m^2)^3} + 2 \frac{(qB^2)p_\perp^2 - (qE)^2(p_2^2 + p_3^2)}{(p^2 + m^2)^4} \\ &- \frac{2(qE)^2m^2}{(p^2 + m^2)^4}. \end{aligned} \quad (26)$$

### III. MASS CORRECTION

There are several quantities that could be analyzed using the propagator derived in the previous section. Perhaps, the most simple case is the analysis of the electromagnetic mass correction, including also temperature

effects valid for the whole range of temperature. Next, we will consider the effective potential, including rings contributions. We remember that we are dealing here with the  $\lambda\phi^4$  theory,

$$\mathcal{L} = (D_\mu\phi)^\dagger D^\mu\phi + \mu^2\phi^\dagger\phi - \frac{\lambda}{4}(\phi^\dagger\phi)^2, \quad (27)$$

where  $\phi$  is a charged scalar field and

$$D_\mu = \partial_\mu + iqA_\mu. \quad (28)$$

The squared mass parameter  $\mu^2$  and the self-coupling  $\lambda$  are taken to be positive. Notice that we are in the broken phase. We can write the complex field  $\phi$  in terms of real components  $\sigma$  and  $\chi$ ,

$$\begin{aligned} \phi(x) &= \frac{1}{\sqrt{2}}[\sigma(x) + i\chi(x)], \\ \phi^\dagger(x) &= \frac{1}{\sqrt{2}}[\sigma(x) - i\chi(x)]. \end{aligned} \quad (29)$$

Following the usual procedure that allows the occurrence of spontaneous symmetry breaking, the  $\sigma$  field develops a vacuum expectation value  $v$

$$\sigma \rightarrow \sigma + v, \quad (30)$$

which can later be taken as the order parameter of the theory. After this shift, the Lagrangian can be rewritten as

$$\begin{aligned} \mathcal{L} &= -\frac{1}{2}[\sigma(\partial_\mu + iqA_\mu)^2\sigma] - \frac{1}{2}\left(\frac{3\lambda v^2}{4} - \mu^2\right)\sigma^2 \\ &- \frac{1}{2}[\chi(\partial_\mu + iqA_\mu)^2\chi] - \frac{1}{2}\left(\frac{\lambda v^2}{4} - \mu^2\right)\chi^2 + \frac{\mu^2}{2}v^2 \\ &- \frac{\lambda}{16}v^4 + \mathcal{L}_I, \end{aligned} \quad (31)$$

where  $\mathcal{L}_I$  is given by

$$\mathcal{L}_I = -\frac{\lambda}{16}(\sigma^4 + \chi^4 + 2\sigma^2\chi^2), \quad (32)$$

From Eq. (31) we see that the  $\sigma$  and  $\chi$  masses are given by

$$\begin{aligned} m_\sigma^2 &= \frac{3}{4}\lambda v^2 - \mu^2, \\ m_\chi^2 &= \frac{1}{4}\lambda v^2 - \mu^2. \end{aligned} \quad (33)$$

For the discussion of the propagator, we will consider only the  $\sigma$  boson mass correction which is given by

$$m_\sigma(T, B, E) = m_0 + \Pi_\sigma(T, B, E), \quad (34)$$

where  $m_0$  is the bare mass of the  $\sigma$  field, being  $m_\sigma(T, B, E)$  the mass at the one loop level, corrected by temperature and the external electromagnetic fields. The Feynman diagrams that contribute to the self-energy of the  $\sigma$  boson are shown in figure Fig. (1). Therefore,

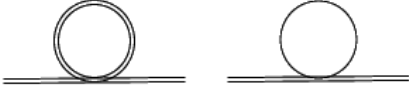


Figure 1. Feynman diagrams that contribute to the self-energy of the  $\sigma$  field. The solid line corresponds to the  $\chi$  field and the double line to the  $\sigma$  field.

the self-energy  $\Pi_\sigma(T, B, E)$  corresponds to

$$\Pi_\sigma(T, B, E) = \frac{\lambda}{4}(12\Pi(m_\sigma) + 2\Pi(m_\chi)), \quad (35)$$

where

$$\Pi(m_i) \equiv \Pi = T \sum_n \int \frac{d^3p}{(2\pi)^3} D(\omega_n, p, m_i), \quad (36)$$

being  $m_i$  the  $\sigma$  or the  $\chi$  mass. Finite temperature effects are handled in the imaginary time formalism in the usual way, i.e.

$$p_4 \rightarrow \omega_n = 2\pi nT, \quad n \in \mathbb{Z}. \quad (37)$$

where the integral in  $p_4$  converts into a sum over Matsubara frequencies according to,

$$\int \frac{d^4p}{(2\pi)^4} f(p) \rightarrow T \sum_{n \in \mathbb{Z}} \int \frac{d^3p}{(2\pi)^3} f(\omega_n, p), \quad (38)$$

where we introduce the notation  $p = (p_1, p_2, p_3)$ . To calculate Eq. (36) in an analytic way, we proceed through the weak field expansion of the propagator up to a quadratic order of Eq. (26) getting

$$\begin{aligned} \Pi &= T \sum_n \int \frac{d^3p}{(2\pi)^3} \left[ \frac{1}{\omega_n^2 + p^2 + m^2} - \frac{4p_2\omega_n(qB)(qE)}{(\omega_n^2 + p^2 + m^2)^4} \right. \\ &\quad - \frac{3(qE)^2 + (qB)^2}{(\omega_n^2 + p^2 + m^2)^3} + 2 \frac{(qB^2)p_1^2 - (qE)^2(p_2^2 + p_3^2)}{(\omega_n^2 + p^2 + m^2)^4} \\ &\quad \left. - \frac{2(qE)^2 m^2}{(\omega_n^2 + p^2 + m^2)^4} \right] \\ &\equiv \Pi_I + \Pi_{II} + \Pi_{III} + \Pi_{IV} + \Pi_V + \Pi_{VI}, \end{aligned} \quad (39)$$

where

$$\begin{aligned} \Pi_I &= T \sum_n \int \frac{d^3p}{(2\pi)^3} \frac{1}{\omega_n^2 + p^2 + m^2} \\ \Pi_{II} &= -T \sum_n \int \frac{d^3p}{(2\pi)^3} \frac{4p_2\omega_n(qB)(qE)}{(\omega_n^2 + p^2 + m^2)^4} \\ \Pi_{III} &= -T \sum_n \int \frac{d^3p}{(2\pi)^3} \frac{3(qE)^2 + (qB)^2}{(\omega_n^2 + p^2 + m^2)^3} \\ \Pi_{IV} &= T \sum_n \int \frac{d^3p}{(2\pi)^3} 2 \frac{(qB^2)p_1^2 - (qE)^2(p_2^2 + p_3^2)}{(\omega_n^2 + p^2 + m^2)^4} \\ \Pi_V &= -T \sum_n \int \frac{d^3p}{(2\pi)^3} \frac{2(qE)^2 m^2}{(\omega_n^2 + p^2 + m^2)^4}. \end{aligned} \quad (40)$$

The first term in the above expression corresponds just to the vacuum plus a thermal contribution. The second term vanishes, due to symmetry reasons, when doing the integral in  $p_2$ . Then we have a sequence of a pure magnetic term followed by a pure electric contribution, a thermomagnetic and, finally, a thermoelectric term. Let us first calculate  $\Pi_I$ ,

$$\begin{aligned} \Pi_I &= T \sum_n \int \frac{d^3p}{(2\pi)^3} \frac{1}{\omega_n^2 + p^2 + m^2} \\ &= \frac{1}{2\pi^2} \int_0^\infty \frac{p^2}{2\sqrt{p^2 + m^2}} (1 + 2n_B(\sqrt{p^2 + m^2})). \end{aligned} \quad (41)$$

We do first the sum over Matsubara frequencies according to [41, 42]

$$\begin{aligned} T \sum_n \frac{1}{(\omega_n^2 + p^2 + m^2)} &= \frac{1}{2\sqrt{p^2 + m^2}} \\ &\times (1 + 2n_B(\sqrt{p^2 + m^2})), \end{aligned} \quad (42)$$

where  $n_B$  is the Bose-Einstein distribution

$$n_B(x) = \frac{1}{e^{x/T} - 1}. \quad (43)$$

The first term in Eq. (41) is handled through the standard renormalization procedure in the  $\overline{\text{MS}}$  scheme, and we obtain

$$\frac{1}{2\pi^2} \int_0^\infty \frac{p^2}{2\sqrt{p^2 + m^2}} = -\frac{m_i^2}{16\pi^2} \left( \ln \left( \frac{\tilde{\mu}^2}{m_i^2} \right) - \frac{1}{2} \right), \quad (44)$$

where  $\tilde{\mu}$  is the ultraviolet renormalization scale. The second term in Eq. (41) is

$$\begin{aligned} &\frac{1}{2\pi^2} \int_0^\infty dp \frac{p^2}{\sqrt{p^2 + m_0^2}} n_B(\sqrt{p^2 + m^2}) \\ &= \frac{1}{2\pi^2} \sum_{n=0}^\infty \int_0^\infty \frac{p^2 e^{-(n+1)\sqrt{p^2 + m^2}/T}}{\sqrt{p^2 + m^2}} \\ &= \frac{mT}{2\pi^2} \sum_{n=1}^\infty \frac{K_1(nm/T)}{n}, \end{aligned} \quad (45)$$

where the modified Bessel function  $K_\alpha(x)$  has the form [43]

$$K_\alpha(x) = \int_0^\infty du e^{-x \cosh(u)} \cosh(\alpha u). \quad (46)$$

It is easy to see that  $\Pi_{II}$  vanishes. Let us proceed now to compute  $\Pi_{III}$ ,

$$\Pi_{III} = -\frac{1}{2} \left( \frac{\partial}{\partial m^2} \right)^2 T \sum_n \int \frac{d^3p}{(2\pi)^3} \frac{3(qE)^2 + (qB)^2}{\omega_n^2 + p^2 + m^2}, \quad (47)$$

where we have employed

$$\frac{(-1)^n}{n!} \left( \frac{\partial}{\partial m^2} \right)^n \frac{1}{\omega_n^2 + p^2 + m^2} = \frac{1}{(\omega_n^2 + p^2 + m^2)^{n+1}}. \quad (48)$$

Making use of the Matsubara frequencies according to Eq. (42), we obtain

$$\Pi_{\text{III}} = -\frac{3(qE)^2 + (qB)^2}{2} \left( \frac{\partial}{\partial m^2} \right)^2 \frac{1}{2\pi^2} \int_0^\infty dp \frac{p^2}{2\sqrt{p^2 + m^2}} \times (1 + 2n_B(\sqrt{p^2 + m^2})). \quad (49)$$

We notice that the first term in the previous expression does not correspond to the vacuum, as it what the case in  $\Pi_{\text{I}}$ . Here we have pure electric and magnetic contributions. The integral can be done using Eq. (46) getting

$$\Pi_{\text{III}} = -(3(qE)^2 + (qB)^2) \left[ \frac{1}{32\pi^2 m^2} + \frac{1}{16\pi^2 m T} \sum_{n=1}^\infty n K_1(nm/T) \right]. \quad (50)$$

In order to calculate  $\Pi_{\text{IV}}$  we use first Eq. (48) with  $n = 3$ , finding

$$\Pi_{\text{IV}} = -\frac{1}{6} \left( \frac{\partial}{\partial m^2} \right)^3 \times T \sum_n \int \frac{d^3 p}{(2\pi)^3} 2 \frac{(qB)^2 p_\perp^2 - (qE)^2 (p_2^2 + p_3^2)}{(\omega_n^2 + p^2 + m^2)}. \quad (51)$$

Due to the symmetry of the integral we can replace  $p_\perp^2 = 2p/3$  y  $p_2^2 + p_3^2 = 2p/3$ , having then

$$\Pi_{\text{IV}} = -\frac{2((qB)^2 - (qE)^2)}{9} \left( \frac{\partial}{\partial m^2} \right)^3 \times T \sum_n \int \frac{d^3 p}{(2\pi)^3} \frac{p^2}{(\omega_n^2 + p^2 + m^2)}. \quad (52)$$

After the sum over Matsubara frequencies we get

$$\Pi_{\text{IV}} = -\frac{((qB)^2 - (qE)^2)}{9\pi^2} \left( \frac{\partial}{\partial m^2} \right)^3 \int_0^\infty dp \frac{p^4}{2\sqrt{p^2 + m^2}} \times (1 + 2n_B(\sqrt{p^2 + m^2})). \quad (53)$$

In an analogous way to the case  $\Pi_{\text{III}}$ , the purely electric and magnetic cases are obtained by calculating the integrals whereas for the temperature dependent case we use Eq. (46), obtaining

$$\Pi_{\text{IV}} = ((qB)^2 - (qE)^2) \left[ \frac{1}{48\pi^2 m^2} - \frac{1}{24\pi^2 m T} \sum_{n=1}^\infty n K_1(nm/T) \right]. \quad (54)$$

Finally, we calculate  $\Pi_{\text{V}}$  using the same procedure as in the previous cases, i.e. using Eq. (48) proceeding then with the sum over Matsubara frequencies. We obtain

$$\Pi_{\text{V}} = -\frac{(qE)^2 m^2}{6\pi^2} \left( \frac{\partial}{\partial m^2} \right)^3 \int_0^\infty dp \frac{p^2}{2\sqrt{p^2 + m^2}} \times (1 + 2n_B(\sqrt{p^2 + m^2})), \quad (55)$$

and using Eq. (46), we have

$$\Pi_{\text{V}} = -(qE)^2 m^2 \left[ \frac{1}{48\pi^2 m^4} + \frac{1}{48\pi^2 m^2 T^2} \sum_{n=1}^\infty n K_2(nm/T) \right]. \quad (56)$$

Putting together all different contributions, we finally obtain

$$\begin{aligned} \Pi = & -\frac{m^2}{16\pi^2} \left( \ln \left( \frac{\tilde{\mu}^2}{m^2} \right) - \frac{1}{2} \right) + \frac{mT}{2\pi^2} \sum_{n=1}^\infty \frac{K_1(nm/T)}{n} \\ & + (qE)^2 \left[ -\frac{13}{96\pi^2 m^2} - \frac{11}{48\pi^2 m T} \sum_{n=1}^\infty n K_1(nm/T) \right. \\ & \left. - \frac{1}{48\pi^2 T^2} \sum_{n=1}^\infty n K_2(nm/T) \right] \\ & + (qB)^2 \left[ -\frac{1}{96\pi^2 m^2} - \frac{1}{48\pi^2 m T} \sum_{n=1}^\infty n K_1(nm/T) \right]. \quad (57) \end{aligned}$$

Using our result for the self-energy correction, we will proceed now to show graphs for Eq. (34). As a reference value for the bare mass we will take the pion mass, i.e.  $m_0 = 140$  MeV. The idea is to graph the evolution of the sigma mass in terms of temperature and the electric and magnetic field intensities. Since in the selfenergy calculation our results are valid for the whole range of temperature values, we will make a graph for the sigma mass as function of temperature (without any restrictions) for different strengths of the magnetic and electric field strengths, staying nevertheless always in the weak sector in both cases. This is shown in Fig. (2). The blue curve represents the temperature mass evolution in absence of electric and magnetic fields. The orange curve corresponds to the case where the electric field vanishes but where the magnetic field has the value of  $0.9m_0^2$ . The green curve corresponds to the opposite case where the magnetic field vanishes and where the electric field has the value of  $0.9m_0^2$ . Finally, the red curve represents the case where both fields have an intensity of  $0.9m_0^2$ . We observe that the mass grows, as we in fact expected, as function of temperature. However, as soon as one of the fields appears on stage this growing behavior becomes less pronounced. In fact, in the low temperature region the mass diminishes. By comparing

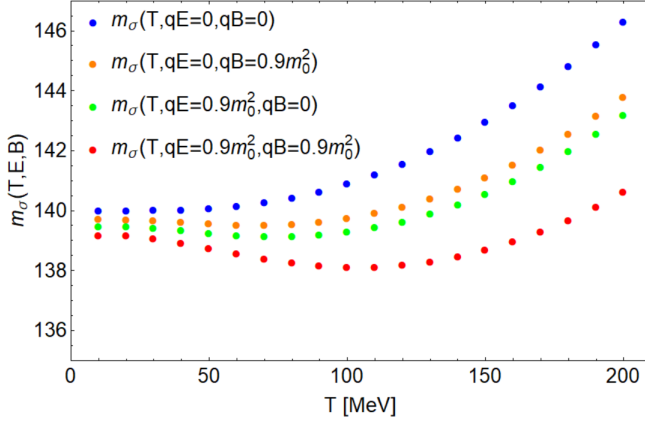


Figure 2. Color on-line. Sigma mass as function of temperature for different strengths of the electric and/or magnetic fields.

the orange and green curves we see that the electric field has a stronger effect in comparison with the magnetic field in diminishing the thermal mass evolution. In the presence of both type of fields, their influence dominates over temperature up to an approximate temperature of  $T = 100$  MeV. For bigger values of temperature the mass starts again to increase as function of temperature.

In order to get a different perspective, we will graph the evolution of the mass as function of the strengths of the fields in the  $T = 0$  case as we can see in Fig. (3). In this case, the blue curve represents the evolution of the sigma mass as function of the magnetic field when the electric field vanishes whereas the opposite case, the evolution of the mass as function of the electric field when the magnetic field vanishes, is represented by the orange curve. Finally, the green curve represents the mass evolution as function of both field intensities. We notice that the mass diminishes as function of the field strengths in both cases (electric or magnetic) being this behavior more relevant in the electric than in the magnetic case. As expected, when both fields are present, the diminishing mass behavior becomes even more evident.

#### IV. EFFECTIVE POTENTIAL

As we said in the previous section, we want also to analyze the effective potential for our  $\lambda\phi^4$  model, including the contribution of ring diagrams, in the presence of a weak electromagnetic external fields and temperature contributions, as well, being these effects valid for the whole range of temperature values.

In our model, the tree level potential is given by

$$V^{(\text{tree})} = -\frac{1}{2}\mu^2 v^2 + \frac{1}{16}\lambda^2 v^4, \quad (58)$$

The effective potential at the one loop level corresponds

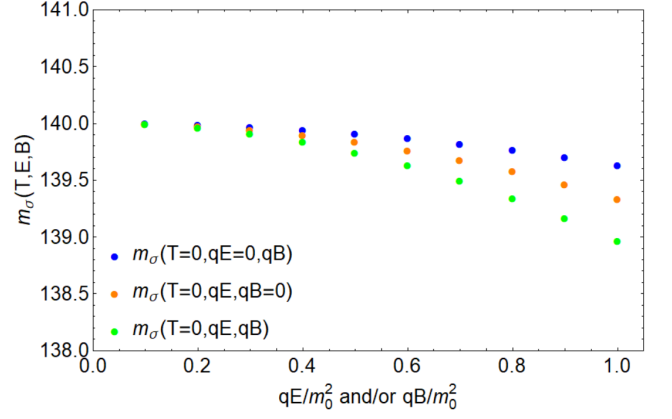


Figure 3. Color on-line. Sigma mass as function of the electric and/or magnetic field for the  $T = 0$  case.

to [41, 42]

$$\begin{aligned} V^{(1\text{-loop})} &= \sum_{i=\sigma,\chi} \left( \frac{T}{2} \sum_n \int \frac{d^3p}{(2\pi)^3} \ln[D(\omega_n, p, m_i)]^{-1} \right) \\ &= \sum_{i=\sigma,\chi} \left( \frac{T}{2} \sum_n \int dm_i^2 \int \frac{d^3p}{(2\pi)^3} D(\omega_n, p, m_i) \right) \\ &\equiv \frac{T}{2} \sum_n \int dm^2 \int \frac{d^3p}{(2\pi)^3} D(\omega_n, p, m), \quad (59) \end{aligned}$$

where in the last equality we denoted  $m_i$  as  $m$ . It is understood that the result corresponds to the sum of both contributions. Using now the propagator according to Eq. (26), we get

$$\begin{aligned} V^{(1\text{-loop})} &= \frac{T}{2} \sum_n \int dm^2 \int \frac{d^3p}{(2\pi)^3} \left[ \frac{1}{\omega_n^2 + p^2 + m^2} \right. \\ &\quad - \frac{4p_2\omega_n(qB)(qE)}{(\omega_n^2 + p^2 + m^2)^4} - \frac{3(qE)^2 + (qB)^2}{(\omega_n^2 + p^2 + m^2)^3} \\ &\quad + 2 \frac{(qB^2)p_\perp^2 - (qE)^2(p_2^2 + p_3^2)}{(\omega_n^2 + p^2 + m^2)^4} \\ &\quad \left. - \frac{2(qE)^2 m^2}{(\omega_n^2 + p^2 + m^2)^4} \right] \\ &\equiv V_I + V_{II} + V_{III} + V_{IV} + V_V + V_{VI}, \quad (60) \end{aligned}$$

where

$$\begin{aligned}
V_I &= \frac{T}{2} \sum_n \int dm^2 \int \frac{d^3 p}{(2\pi)^3} \frac{1}{\omega_n^2 + p^2 + m^2} \\
V_{II} &= -\frac{T}{2} \sum_n \int dm^2 \int \frac{d^3 p}{(2\pi)^3} \frac{4p_2 \omega_n (qB)(qE)}{(\omega_n^2 + p^2 + m^2)^4} \\
V_{III} &= -\frac{T}{2} \sum_n \int dm^2 \int \frac{d^3 p}{(2\pi)^3} \frac{3(qE)^2 + (qB)^2}{(\omega_n^2 + p^2 + m^2)^3} \\
V_{IV} &= \frac{T}{2} \sum_n \int dm^2 \int \frac{d^3 p}{(2\pi)^3} 2 \frac{(qB)^2 p_\perp^2 - (qE)^2 (p_2^2 + p_3^2)}{(\omega_n^2 + p^2 + m^2)^4} \\
V_V &= -\frac{T}{2} \sum_n \int dm^2 \int \frac{d^3 p}{(2\pi)^3} \frac{2(qE)^2 m^2}{(\omega_n^2 + p^2 + m^2)^4}. \quad (61)
\end{aligned}$$

The procedure is analogous to the previous calculation. For the case  $V_I$  we have a vacuum contribution and an exclusively thermal part obtaining in the  $\overline{\text{MS}}$  scheme,

$$V_I = -\frac{m^4}{64\pi^2} \left( \ln \left( \frac{\tilde{\mu}^2}{m^2} \right) + \frac{3}{2} \right) - \frac{m^2 T^2}{2\pi^2} \sum_{n=1}^{\infty} \frac{K_2(nm/T)}{n^2}. \quad (62)$$

The case  $V_{II} = 0$  due to the integral in  $dp_2$  and for the case  $V_{III}$  we have

$$V_{III} = (3(qE)^2 + (qB)^2) \times \left[ \frac{1}{64\pi^2} \ln \left( \frac{\tilde{\mu}^2}{m^2} \right) + \frac{1}{16\pi^2} \sum_{n=1}^{\infty} n K_0(nm/T) \right]. \quad (63)$$

Using the same strategy employed for the term  $\Pi_{IV}$ , for  $V_{IV}$  we obtain

$$\begin{aligned}
V_{IV} &= ((qE)^2 - (qB)^2) \\
&\times \left[ \frac{1}{96\pi^2} \ln \left( \frac{\tilde{\mu}^2}{m^2} \right) - \frac{1}{144\pi^2} - \frac{1}{24\pi^2} \sum_{n=1}^{\infty} n K_0(nm/T) \right]. \quad (64)
\end{aligned}$$

Finally, for  $\Pi_V$ , we get

$$\begin{aligned}
\Pi_V &= (qE)^2 \left[ \frac{1}{96\pi^2} \ln \left( \frac{\tilde{\mu}^2}{m^2} \right) + \frac{1}{96\pi^2} \right. \\
&+ \left. \frac{1}{24\pi^2} \sum_{n=1}^{\infty} \frac{K_0(nm/T)}{n} + \frac{m}{48\pi^2 T} \sum_{n=1}^{\infty} K_1(nm/T) \right]. \quad (65)
\end{aligned}$$

The sum of all contributions gives us finally the one loop effective potential

$$\begin{aligned}
V^{(1\text{-loop})} &= \sum_{i=\sigma, \chi} \left( -\frac{m_i^4}{64\pi^2} \left( \ln \left( \frac{\tilde{\mu}^2}{m_i^2} \right) + \frac{3}{2} \right) \right. \\
&- \frac{m^2 T^2}{2\pi^2} \sum_{n=1}^{\infty} \frac{K_2(nm/T)}{n^2} + (qE)^2 \left[ \frac{13}{192\pi^2} \ln \left( \frac{\tilde{\mu}^2}{m_i^2} \right) \right. \\
&+ \frac{1}{288\pi^2} + \frac{11}{48\pi^2} \sum_{n=1}^{\infty} n K_0(nm_i/T) \\
&+ \frac{1}{24\pi^2} \sum_{n=1}^{\infty} \frac{K_0(nm_i/T)}{n} + \frac{m}{48\pi^2 T} \sum_{n=1}^{\infty} K_1(nm_i/T) \left. \right] \\
&+ (qB)^2 \left[ \frac{1}{192\pi^2} \ln \left( \frac{\tilde{\mu}^2}{m_i^2} \right) - \frac{1}{144\pi^2} \right. \\
&+ \left. \left. \frac{1}{48\pi^2} \sum_{n=1}^{\infty} n K_0(nm_i/T) \right] \right]. \quad (66)
\end{aligned}$$

### A. The ring potential

The ring contribution is given by [41, 42]

$$V^{(\text{ring})} = \frac{T}{2} \sum_n \int \frac{d^3 p}{(2\pi)^3} \ln[1 + \Pi(\omega_n, p) D(\omega_n, p)]. \quad (67)$$

The previous expression can be written as

$$\begin{aligned}
V^{(\text{ring})} &= \frac{T}{2} \sum_n \int \frac{d^3 p}{(2\pi)^3} \ln[(D(\omega_n, p)^{-1} + \Pi(\omega_n, p)) \\
&\times (D(\omega_n, p))] \\
&= \frac{T}{2} \sum_n \int \frac{d^3 p}{(2\pi)^3} \ln[D(\omega_n, p)] \\
&+ \frac{T}{2} \sum_n \int \frac{d^3 p}{(2\pi)^3} \ln[D(\omega_n, p)^{-1} + \Pi(\omega_n, p)], \quad (68)
\end{aligned}$$

Notice that by considering the sum of the one loop contributions and the rings, we get

$$\begin{aligned}
V^{(1\text{-loop})} + V^{(\text{ring})} &= \frac{T}{2} \sum_n \int \frac{d^3 p}{(2\pi)^3} \ln[D(\omega_n, p)^{-1} \\
&+ \Pi(\omega_n, p)]. \quad (69)
\end{aligned}$$

Therefore, it is not necessary to calculate something else. In fact, we have just to replace the mass  $m^2$  by  $m^2 + \Pi$  in Eq. (66). The expression for the effective potential up to ring order is given by

$$\begin{aligned}
& V^{(\text{tree})} + V^{(1\text{-loop})} + V^{(\text{ring})} = \\
& -\frac{1}{2}\mu^2 v^2 + \frac{1}{16}\lambda^2 v^4 \\
& \sum_{i=\sigma,\chi} \left( -\frac{(m_i^2 + \Pi)^2}{64\pi^2} \left[ \ln \left( \frac{\tilde{\mu}^2}{m_i^2 + \Pi} \right) + \frac{3}{2} \right] \right. \\
& - \frac{(m_i^2 + \Pi)T^2}{2\pi^2} \sum_{n=1}^{\infty} \frac{K_2(n\sqrt{m_i^2 + \Pi}/T)}{n^2} \\
& + (qE)^2 \left[ \frac{13}{192\pi^2} \ln \left( \frac{\tilde{\mu}^2}{m_i^2 + \Pi} \right) + \frac{1}{288\pi^2} \right. \\
& + \frac{11}{48\pi^2} \sum_{n=1}^{\infty} n K_0(n\sqrt{m_i^2 + \Pi}/T) \\
& + \frac{1}{24\pi^2} \sum_{n=1}^{\infty} \frac{K_0(n\sqrt{m_i^2 + \Pi}/T)}{n} \\
& + \left. \frac{\sqrt{m_i^2 + \Pi}}{48\pi^2 T} \sum_{n=1}^{\infty} K_1(n\sqrt{m_i^2 + \Pi}/T) \right] \\
& + (qB)^2 \left[ \frac{1}{192\pi^2} \ln \left( \frac{\tilde{\mu}^2}{m_i^2 + \Pi} \right) - \frac{1}{144\pi^2} \right. \\
& + \left. \frac{1}{48\pi^2} \sum_{n=1}^{\infty} n K_0(n\sqrt{m_i^2 + \Pi}/T) \right] \Bigg), \quad (70)
\end{aligned}$$

where  $\Pi$  is given by Eq. (57). We stress that the inclusion of rings is crucial for the analyticity of the effective potential, avoiding the appearance of imaginary mass terms. If we want to determine the critical temperature where the symmetry is restored, we need to explore the behavior of the effective potential as function of the expectation value ( $v$ ). It becomes more flat for a growing temperature. At the critical temperature the first and second derivatives, in fact, all derivatives, vanish becoming then convex for  $T > T_c$ . Here we have to do with a second order phase transition since in the whole procedure no degenerated vacuums appear. We obtain, then, the behavior of the critical temperature as function of the strengths of the electromagnetic fields which is shown in Fig. (4). The blue curve is for the case of only an external magnetic field finding IMC. The red curve is for the case of a pure electric field having IEC. The orange curve corresponds to the situation where both fields are present showing the occurrence of IMEC. The inverse catalysis effect becomes more pronounced for the electric field case (red curve) in comparison with the effect induced by only a magnetic field (the blue curve). When both fields are present, the IMEC effect becomes more relevant. It is clear that the electric field has a prominent role, compared with the magnetic case, for the appearance of inverse catalysis.

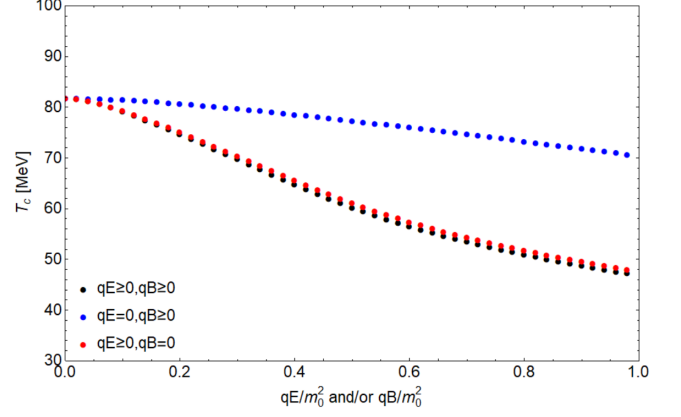


Figure 4. Color on-line. Critical temperature as function of the fields. The black curve corresponds to the case where both fields are present. The red curve is for the case where we have only an electric field and the blue curve corresponds to the case where only a magnetic field is present.

## V. CONCLUSIONS

The main novelty of this work is the derivation of a bosonic propagator in a proper time representation, when external constant magnetic and electric fields are simultaneously present in a perpendicular configuration. Since this propagator is quite cumbersome, in order to get analytical results we have presented a weak field approximation which makes possible to get analytic results for mass corrections and for the effective potential due to the electric and magnetic field effects, including also temperature in the discussion. We worked in the frame of a complex scalar self-interacting field theory. Our results for the mass correction were presented in figures (2) and (3). It turns out that this mass, identified with the sigma mass, grows with temperature whereas the external fields, magnetic and/or electric, tend to diminish it. This opposite behavior between the role of temperature and the role of the external electromagnetic fields, in this case for the mass evolution, was also observed in other scenarios as, for example, in the determination of scattering lengths or the behavior of renormalon residues [44–47]. From Fig. (3) we notice that when temperature vanishes, the sigma mass diminishes as function of the external fields being this behavior more significant for an electric external field than in the case of a magnetic field.

As an important conclusion about the effective potential, we want to stress the occurrence of IMC or IEC for the cases where only a magnetic field or only an electric field are present, respectively. IMEC was clearly found, when both fields are simultaneously present, cooperating both fields for the IMEC effect. We have shown that the electric field plays a more important role, with respect to the magnetic field influence, for the decreasing of the critical temperature. Although we have used a quite simple model, the central result, namely the explicit propagator in the presence of external electric and/or magnetic

fields, could be used in more realistic scenarios as, for example, the linear sigma model. We would like to explore this case in a future work.

### ACKNOWLEDGEMENTS

M. Loewe and R. Zamora acknowledge support from ANID/CONICYT FONDECYT Regular (Chile) under

Grants No. 1200483 and 1220035. M.L. acknowledges support from FONDECYT Regular under grant No. 1190192. ML acknowledges also support from ANID PIA/APOYO AFB 180002 (Chile).

- 
- [1] Sh. Fayazbakhsh and N. Sadooghi, *Phys. Rev. D* **88**, 065030 (2013).
  - [2] A. Ayala, J.L. Hernández, L. A. Hernández, R.L.S Farias and R. Zamora, *Phys. Rev. D* **103**, 054038 (2021).
  - [3] A. Ayala, J.L. Hernández, L. A. Hernández, R.L.S Farias and R. Zamora, *Phys. Rev. D* **102**, 114038 (2020).
  - [4] C.A. Dominguez, L. A. Hernández, M. Loewe, C. Villavicencio and R. Zamora, *Phys. Rev. D* **102**, 094007 (2020).
  - [5] Yu. A. Simonov, *Phys. At. Nucl.* **79**, 455 (2016).
  - [6] R. M. Aguirre, *Eur. Phys. J. A* **55**, 28 (2019).
  - [7] T. Yoshida and K. Suzuki, *Phys. Rev. D* **94**, 074043 (2016).
  - [8] D. Dudal and T. G. Mertens, *Phys. Rev. D* **91**, 086002 (2015).
  - [9] K. Marasinghe and K. Tuchin, *Phys. Rev. C* **84**, 044908 (2011).
  - [10] P. Gubler, K. Hattori, S. H. Lee, M. Oka, S. Ozaki and K. Suzuki, *Phys. Rev. D* **93**, 054026 (2016).
  - [11] C. S. Machado, S. I. Finazzo, R. D. Matheus and J. Noronha, *Phys. Rev. D* **89**, 074027 (2014).
  - [12] S. Cho, K. Hattori, S. H. Lee, K. Morita and S. Ozaki, *Phys. Rev. Lett.* **113**, 172301 (2014).
  - [13] A. Ayala, R. L. S. Farias, S. Hernández-Ortíz, L. A. Hernández, D. Manreza Paret and R. Zamora, *Phys. Rev. D* **98**, 114008 (2018).
  - [14] S. Cho, K. Hattori, S. H. Lee, K. Morita and S. Ozaki, *Phys. Rev. D* **91**, 045025 (2015).
  - [15] S. Ghosh, A. Mukherjee, M. Mandal, S. Sarkar and P. Roy, *Phys. Rev. D* **94**, 094043 (2016).
  - [16] A. Bandyopadhyay and S. Mallik, *Eur. Phys. J. C* **77**, 771 (2017).
  - [17] S. S. Avancini, W. R. Tavares and M. B. Pinto, *Phys. Rev. D* **93**, 014010 (2016).
  - [18] S. S. Avancini, R. L. Farias, M. B. Pinto, W. R. Tavares and V. S. Timteo, *Phys. Lett. B* **767**, 247 (2017).
  - [19] A. Ayala, C. A. Dominguez, L. A. Hernández, M. Loewe and R. Zamora, *Phys. Rev. D* **92**, 096011 (2015).
  - [20] A. Ayala, S. Hernandez-Ortiz, L. A. Hernandez, V. Knapp-Perez and R. Zamora, *Phys. Rev. D* **201**, 074023 (2020).
  - [21] M. Ruggieri and G. X. Peng, *Phys. Rev. D* **93**, 094021 (2016).
  - [22] D. Cohen, D. A. McGady, and E. S. Werbos, *Phys. Rev. C* **76**, 055201 (2007).
  - [23] W. R. Tavares and S. S. Avancini, *Phys. Rev. D* **97**, 094001 (2018).
  - [24] Pedro Costa, Márcio Ferreira, Débora P. Menezes, João Moreira, and Constança Providência, *Phys. Rev. D*, **92**, 036012 (2015).
  - [25] Jens O. Andersen, *Eur. Phys. J. A* (2021) 57: 189.
  - [26] A. Ahmad and A. Raya, *J. Phys. G* **43**, 065002, 2016.
  - [27] M. Ferreira, P. Costa, O. Lourenço, T. Fredetico and C. Providência, *Phys. Rev. D*, **89**, 116011 (2014).
  - [28] A. Ayala, L. A. Hernández, M. Loewe, J. C. Rojas and R. Zamora, *Eur. Phys. J. A* **56**, (2020).
  - [29] V. A. Miransky and I. A. Shovkovy, *Phys. Rept.* **576**, 1 (2015); D. Kharzeev, K. Landsteiner, A. Schmitt, Ho-Ung Yee, Editors, *Strongly Interacting Matter in Magnetic Fields*, © Springer-Verlag Berlin Heidelberg 2013, and references therein. G. Baym, T. Hatsuda, T. Kojo, P.D. Powell, Y. Song, and T. Takasuka, *Rept. Prog. Phys.* **81** (2018) 5, 056902; D. Blaschke, A. Ayriyan, and A. Friesen (Editors), “Compact Stars in the QCD Phase Diagram”, Universe, MppiaG (2020).
  - [30] G. S. Bali, F. Bruckmann, G. Endrödi, Z. Fodor, S. D. Katz and A. Schäfer, *Phys. Rev. D* **86**, 071502 (2012); G. Bali, F. Bruckmann, G. Endrödi, Z. Fodor, S. Katz, S. Krieg, A. Schaefer, and K. K. Szabo, *JHEP* **1202**, 044 (2012); G. Bali, F. Bruckmann, G. Endrödi, S. Katz, and A. Schäfer, *JHEP* **1408**, 177 (2014).
  - [31] A. Ayala, M. Loewe and R. Zamora, *Phys. Rev. D* **91**, 016002 (2015);
  - [32] A. Ayala, M. Loewe, A. Mizher and R. Zamora, *Phys. Rev. D* **90**, 036001 (2014).
  - [33] Alejandro Ayala, Luis. A. Hernández, Marcelo Loewe, and Cristian Villavicencio, *Eur. Phys. J. A* **57** (2021), 7, 234.
  - [34] M. Loewe, D. Valenzuela and R. Zamora, *Phys. Rev. D* **105**, 036017 (2022).
  - [35] W. R. Tavares, R. L. S. Farias and S. S. Avancini, *Phys. Rev. D* **101**, 016017 (2020).
  - [36] M. Loewe and R. Zamora, *Phys. Rev. D* **105**, 076011 (2022).
  - [37] G. Cao and X.G. Huang, *Phys. Rev. D* **93**, 016007 (2016); M. Ruggieri, and G. X. Peng, *Phys. Rev. D* **93**, 094021 (2016); M. Ruggieri, Z. Y. Lu and G. X. Peng, *Phys. Rev. D* **94**, 116002 (2016).
  - [38] Walter Dittrich and Martin Reuter, “Effective Lagrangian in Quantum Electrodynamics”. Springer-Verlag, Berlin Heidelberg New York, Tokyo (1985). See also Walter Dittrich and Holger Gies, “Probing the Quantum Vacuum: Perturbative effective action approach in Quantum Electrodynamics and its application”, Springer Tracts in Modern Physics, Volume 166 (2000)
  - [39] A. Ahmad, N. Ahmadiaz, O. Corradini, S. P. Kim and C. Schubert, *Nuclear Physics B*, **919** (2017).
  - [40] A. Ayala, J. Castaño, L. A. Hernandez, J. Salinas and R. Zamora, *Eur. Phys. J. A* **57**, (2021).

- [41] M. Le Bellac, *Thermal Field Theory*, Cambridge University Press, 1996.
- [42] J. I. Kapusta and C. Gale, *Finite-Temperature Field Theory Principles and Applications*, Cambridge University Press, 2006.
- [43] Abramowitz, M. and Stegun, I. A. (Eds.). *Handbook of Mathematical Functions with Formulas, Graphs, and Mathematical Tables*, 9th printing. New York: Dover, pp. 576-579, 1972.
- [44] M. Correa, M. Loewe and R. Zamora, *Phys. Rev. D* **99**, 096024 (2019).
- [45] M. Loewe, L. Monje and R. Zamora, *Phys. Rev. D* **104**, 016020 (2021).
- [46] M. Loewe, E. Muñoz and R. Zamora, *Phys. Rev. D* **100**, 116006 (2019).
- [47] M. Loewe, L. Monje, E. Muñoz, A. Raya and R. Zamora, *Phys. Rev. D* **99**, 056002 (2019).